

O. Naggara
F. Louillet
E. Touzé
D. Roy
X. Leclerc
J.-L. Mas
J.-P. Pruvo
J.-F. Meder
C. Oppenheim

Added Value of High-Resolution MR Imaging in the Diagnosis of Vertebral Artery Dissection

BACKGROUND AND PURPOSE: The optimal imaging method for the diagnosis of VAD remains undefined. Our aim was to evaluate the added value of HR-MR imaging for the diagnosis of VAD.

MATERIALS AND METHODS: We retrospectively extracted 35 consecutive patients suspected of having acute VAD who had the following: 1) a focal lumen abnormality of the VA on CE-MRA, 2) HR-MR imaging during the initial hospital stay, and 3) clinical and imaging follow-up within 6 months. Two neurologists classified patients as either VAD (group A) or non-VAD (group B) by reviewing all the available data at hospital discharge, except HR-MR imaging data. On HR-MR imaging, 2 radiologists searched for signs of acute VAD. The 2 classifications were compared. In case of discordance, CE-MRA follow-up and axial fat-suppressed T1WI, used to obtain supportive evidence for or against VAD, were considered as the standard of reference.

RESULTS: In 4/18 patients in group A, HR-MR imaging did not demonstrate any signs of acute VAD and perivertebral signal-intensity changes were attributed to venous plexus, with an unchanged lumen on follow-up. In 4/17 patients in group B, HR-MRI demonstrated a mural hematoma, with lumen normalization on follow-up CE-MRA.

CONCLUSIONS: Our results encourage the use of HR-MR imaging as a second-line diagnostic tool in the event of suspicion of acute VAD and doubtful findings on standard imaging.

ABBREVIATIONS: CE-MRA = contrast-enhanced MR angiography; CI = confidence interval; DSA = digital subtraction angiography; DUS = Doppler ultrasonography examination; DWI = diffusion-weighted imaging; HR = high resolution; NIHSS = National Institutes of Health Stroke Scale; PDWI = proton attenuation-weighted imaging; T1WI = T1-weighted imaging; T2WI = T2-weighted imaging; TE_{eff} = effective echo-time; TOF = time of flight; V2 and V3 = the second and third VA segments; VA = vertebral artery; VAD = VA dissection

VAD is a diagnostic challenge. The diagnosis is generally based on a suggestive clinical presentation, exclusion of atherosclerosis, and supportive radiologic evidence.¹⁻⁴ An early and reliable diagnosis is important because anticoagulation or antithrombotic treatment is recommended to reduce the risk of a thromboembolic event occurring within the first few days after dissection.⁵ The optimal imaging method for the diagnosis of VAD is still debated.¹ DUS, the first-line screening tool for assessing patients suspected of having acute dissection,³ may show normal findings as long as the mural hematoma results in subtle lumen alterations or is located in a segment that cannot readily be displayed by DUS.⁶ Despite the ability of CT angiography to reveal imaging findings of VAD,⁷ brain CT is known to be poorly sensitive for the detection of posterior fossa ischemic lesions. Thus, cervical CE-MRA coupled with T1WI fat-suppressed axial sequences has gradually replaced conventional angiography for the diagnosis of cervical artery dissection.⁸ However, the proximity of the bone, the tortuous course of the VA associated with the great variability

in normal vessel caliber, and the small size of the mural hematoma in VAD contribute to the difficulty of making a reliable diagnosis. The main pitfall is that a perivertebral venous plexus can mimic the crescent signal-intensity changes of the mural hematoma. Consequently, it is not rare for the diagnosis of VAD to remain presumptive despite an extensive imaging work-up. The diagnosis can be retrospectively confirmed on imaging follow-up by monitoring the lumen healing or progression in response to treatment.

HR-MR imaging is a noninvasive imaging technique that provides a delineation of the lumen and arterial wall.⁹ This technique, which requires dedicated surface coils, has been used extensively for carotid atherosclerosis and, more recently, for carotid dissection.¹⁰⁻¹² Except for 1 case study,¹³ there are no data in the literature that support a role for HR-MR imaging in the diagnosis of VAD. Our aim was to assess the added value of HR-MR imaging for this purpose. Given the absence of a criterion standard for this diagnosis, we could not design a sensitivity/specificity study. We consequently compared the conclusions based on a standard etiologic work-up with those based on HR-MR imaging. We expected HR-MR imaging to detect more VAD cases; and conversely, we expected the findings to be normal in some cases with erroneous VAD diagnosis due to perivertebral venous plexus. In case of discordance between HR-MR imaging and the standard etiologic work-up, we used the serial imaging follow-up to obtain supportive evidence for or against VAD and considered it as a criterion standard.

Received November 12, 2009; accepted after revision April 5, 2010.

From the Departments of Neuroradiology (O.N., J.-F.M., C.O.) and Neurology (F.L., E.T., J.-L.M.), Paris-Descartes University, Institut national de la santé et de la recherche médicale U894, Centre Hospitalier Sainte-Anne, Paris, France; Interventional Neuroradiology Research Unit (O.N., D.R.), Centre Hospitalier de l'Université de Montréal, Notre-Dame Hospital, University of Montreal, Quebec, Canada; and Department of Neuroradiology (J.-P.P., X.L.), Lille University Hospital Roger Salengro, Lille, France.

Please address correspondence to Olivier Naggara, MD, Department of Neuroradiology, Centre Hospitalier Sainte-Anne, 1 rue Cabanis, 75014 Paris, France; e-mail: o.naggara@ch-sainte-anne.fr

DOI 10.3174/ajnr.A2165

Materials and Methods

Patients

The study was approved by our local ethics committee and was found to conform to generally accepted scientific principles and research ethics standards. From our stroke center imaging data base (January 2007 to April 2008), which includes in- and outpatient settings, we retrospectively extracted 70 consecutive patients in whom cervical axial fat-suppressed T1WI and CE-MRA were performed during the same imaging session. This population comprised all patients clinically suspected of having a cervical dissection, given that these 2 sequences are systematically used to search for mural hematoma and lumen stenosis. From this population, we excluded 28 patients suspected of having acute carotid artery dissection to minimize bias during the reading sessions and to avoid artificially increasing the specificity of HR-MR imaging for the diagnosis of VAD by increasing the number of true-negative cases. From the remaining 42 patients, we selected those with the following: 1) lumen CE-MRA abnormality (ranging from minimal irregularity to occlusion) of at least 1 VA; 2) HR-MR imaging during the initial hospital stay, focused on lumen CE-MRA abnormality; and 3) clinical and MR imaging follow-up. Seven patients had no VA focal lesion on CE-MRA and were then excluded from the study because it was impossible to define a level of exploration for HR-MR imaging.

Standard Imaging Protocol

Standard MR Imaging. Standard MR imaging, which combined investigation of both neck and brain, was performed on a 1.5T whole-body scanner (Signa HDx; GE Healthcare, Milwaukee, Wisconsin) within 48 hours after admission. The neck imaging protocol consisted of at least a fast spin-echo T1WI fat-suppressed axial sequence (FOV, 200 × 200 mm; acquisition matrix, 288 × 256; 2 excitations; 5-mm section thickness; 1.5-mm intersection gap; 16 sections; TR, 600 ms; TE_{eff}, 8.1 ms; scanning time, 3 minutes 59 seconds), followed by CE-MRA of brain-supplying arteries (intravenous meglumine gadoterate, Dotarem; Guerbet, Aulnay-sous-Bois, France; 0.1 mmol/kg body weight; FOV, 260 × 260 mm; acquisition matrix, 416 × 256; 1 excitation; 1.2 mm thick; 0.6-mm gap; TR, 4.9 ms; TE_{eff}, 1.5 ms; scanning time, 82 seconds) by using an 8-channel phased-array coil for head and neck imaging.

HR-MR Imaging

Acquisition. HR-MR images were acquired on a 1.5T MR imaging unit (Signa, GE Healthcare), by using a pair of dedicated phased-array surface coils with 4 circular elements (PACC-GS15, Machnet BV, Eelde, the Netherlands) placed bilaterally on the upper and posterior part of the neck, allowing contemporaneous imaging of both vertebral arteries. The HR-MR imaging protocol combined 4 pulse sequences: T1WI, fat-suppressed PDWI, fat-suppressed T2WI, and 3D TOF angiography. The TOF sequence was centered on the presumed level of the VAD, based on initial DUS, standard axial fat-suppressed T1WI, and CE-MRA. Several levels were imaged with a TOF sequence in case of discordance between DUS, standard axial fat-suppressed T1WI, and CE-MRA for the position of the suspected VAD. The z-axis coordinates of the suspected mural hematoma or irregular lumen as determined on native TOF images were further used to position the 3 other pulse sequences. When a dissection was suspected of involving V3, sequences were acquired in the oblique plane, perpendicular to the V3 segment. The FOV (130 × 130 mm) was identical for all 4 sequences. T1WI, T2WI, and PDWI were per-

formed with double inversion recovery (ie, black-blood) fast spin-echo sequences with electrocardiographic gating during free breathing by using 8–12 axial sections (3-mm section thickness; 1.3-mm intersection gap; mean longitudinal coverage, 39.6 mm; range, 34.4–51.6 mm). PDWI and T2WI parameters were the following: TR, 2 RR intervals; TE_{eff}, 16–20 ms for PDWI and 50 ms for T2WI; acquisition matrix, 256 × 256; 512 mm with zero-filling; in-plane resolution, 0.254 × 0.254 mm; signal-intensity averaged, 2; fat suppression. T1WI parameters were the following: TR, 1 RR interval; TE, 9–10 ms; acquisition matrix, 352 × 256; in-plane resolution, 0.369 × 0.508 mm; signal intensity averaged, 3. The 3D TOF sequence used a gradient-echo pulse sequence with the following parameters: TR, 30 ms; TE, 6.9 ms; flip angle, 20°, acquisition matrix, 288 × 224; 512 mm with zero-filling; in-plane resolution, 0.254 × 0.254 mm; signal intensity averaged, 2; 20 sections of 2.2-mm thickness; 1 slab. Total acquisition time was approximately 30 minutes. Images in DICOM format were anonymized for analysis.

Image Analysis

Neurologists' Classification. Two senior stroke neurologists (F.L., E.T.) independently assigned each patient to either the VAD group (group A) or the non-VAD group (group B), after reviewing all clinical and paraclinical investigations available at hospital discharge (DUS, initial brain MR imaging, CE-MRA, axial fat-suppressed T1WI, and etiologic cardiac and biologic work-ups). Cases of discordance were resolved by consensus. Before the classification, a third author (O.N.) anonymized (name, length and period of stay, date of birth, address, general physician) and extensively expunged all information (HR-MR imaging data, conclusions, treatment, outcome, follow-up data, destination after discharge) from the records that might have biased the neurologists' interpretation. Moreover, reading sessions were performed 1 and 2 years after the inclusion of the last patient, thus minimizing recall bias. Neurologists assigned to group A all patients with a clinical and paraclinical presentation suggestive of VAD, with crescentic hyperintense thickening suggestive of mural hematoma on axial fat-suppressed T1WI. All other patients were assigned to group B.

HR-MR Imaging Classification. Two senior neuroradiologists (O.N., C.O.), blinded to the neurologists' classification and imaging follow-up but aware that patients had been referred with suspected VAD, independently reviewed all anonymized HR-MR images on a dedicated workstation (Advantage for Windows 4.4, GE Healthcare). They looked for signs of recent VAD: 1) pseudoaneurysm, 2) double lumen, and 3) crescentic high-signal intensity of the vertebral wall on all sequences brighter than that of the sternocleidomastoid muscle associated with a signal-intensity loss of the layer between the lumen and the crescentic hyperintense mural thickening on the TOF sequence. This latter pattern, related to inherent magnetic susceptibility artifacts, is suggestive of recent bleeding (Fig 1).¹⁴ HR-MR imaging was considered nontypical of recent VAD when none of the above-mentioned specific signs were noticed. Moreover, whenever a crescentic high signal intensity of the vertebral wall was seen on T2WI, PDWI, and TOF but not on the T1WI sequence and whenever the low signal intensity of the intimal layer was lacking on the TOF sequence, perivertebral signal-intensity changes were attributed to a prominent venous plexus (Fig 1). Discordance between radiologists was resolved by consensus. To assess intraobserver reproducibility, 1 reader re-examined all image sets 3 months later. In cases of multiple VAD, only the symptomatic VAD, according to local symptoms (ie, cervical pain), was considered.

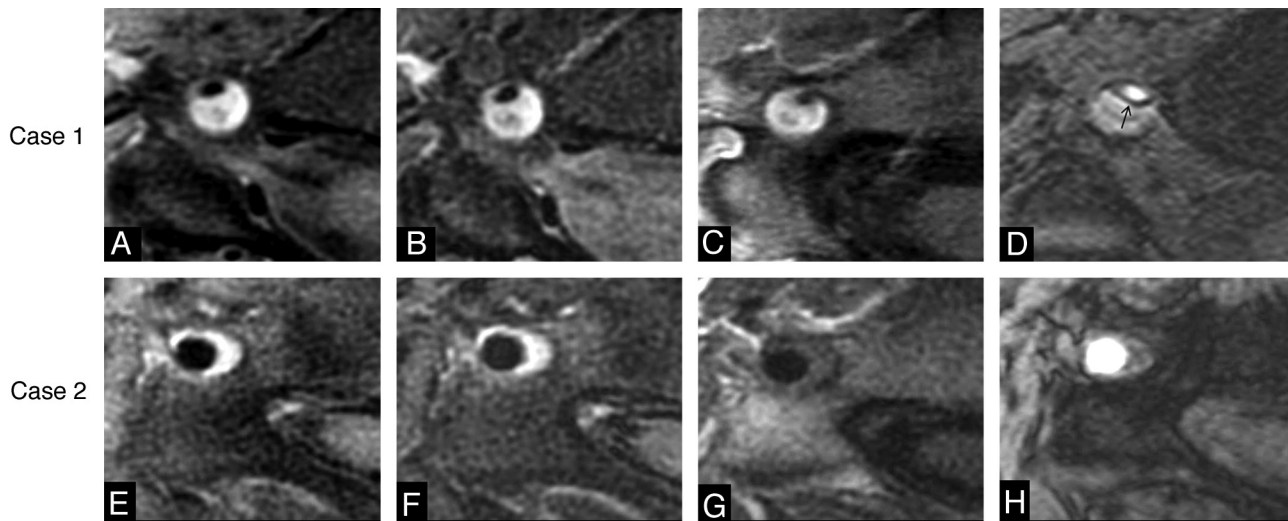


Fig 1. Distinction between mural hematoma and perivertebral hypertrophic venous plexus on HR-MR imaging. Axial high-resolution fat-suppressed PDWI (A and E), fat-suppressed T2WI (B and F), T1WI (C and G), and TOF sequences (D and H). In case 1 (top row), crescentic high signal intensity of the vertebral wall, brighter than the signal intensity of the sternocleidomastoid muscle on all sequences (A–D), is associated with a low signal intensity of the intimal layer between the lumen and the crescentic hyperintense mural thickening on TOF (D, arrow), corresponding to a mural hematoma. In case 2 (bottom row), crescentic high signal intensity of the vertebral wall, brighter than muscle signal intensity on TOF, PDWI, and T2WI (E, F, and H), is isointense to the muscle on T1WI (G), without magnetic susceptibility artifacts (H), leading to the diagnosis of inflow enhancement of a hypertrophic venous structure.

Imaging Follow-Up

Blinded to the neurologists' and the HR-MR imaging classification, we searched for additional supportive evidence for VAD by analyzing the imaging follow-up (mean, 7.4 ± 6.3 months; range, 4–32 months). On follow-up CE-MRA and standard fat-suppressed T1WI, a partial or complete healing of the initial lumen abnormality, an evolution toward a pseudoaneurysm, and a regression of the crescentic mural hyperintense thickening favored the diagnosis of VAD. An unchanged mural thickening favored the diagnosis of hypertrophic venous plexus. No clear conclusion was drawn when the lumen aspect was unchanged during the follow-up period. However, in such a case, VAD was considered unlikely, though it could not be ruled out with certainty.

Statistical Analysis

Inter- and intraobserver agreement for the identification of VAD on HR-MR imaging and interobserver agreement for the neurologists' classification were assessed by calculating κ coefficients and their 95% CIs. We compared the neurologists' groups (A or B) and HR-MR imaging results for each patient.

Results

Interobserver agreement between neurologists was excellent for the diagnosis of VAD ($\kappa = 0.94$; 95% CI, 0.50–0.97). Among the 35 patients (Table 1) suspected of having acute VAD (21 women, 60%; mean age, 41.5 ± 8.5 years; range, 25–56 years), the neurologists assigned 18 to the VAD group (group A) and 17 to the non-VAD group (group B).

On HR-MR imaging, inter- and intraobserver agreement was excellent for the diagnosis of VAD ($\kappa = 0.88$; 95% CI, 0.51–0.94 and $\kappa = 0.92$; 95% CI, 0.50–0.96, respectively). After consensus, HR-MR imaging corroborated the neurologists' classification in 27 (77%) patients (Table 2). HR-MR imaging was suggestive of VAD in 14 of the 18 patients in group A. In 4 of the 18 patients in group A, HR-MR imaging findings were considered normal and periluminal signal-intensity changes were attributed to a hypertrophic periverte-

Table 1: Demographic and clinical data

Demographic Data	
Patients	35
Age (yr, mean, range)	41.5 ± 8.5 (25–56)
Male	14 (40%)
Migraine	14
Diabetes	1
Smoking	19
Hypercholesterolemia	4
Elevated blood pressure	2
Clinical presentation	
Trauma	15
Vertebral manipulation	3
Headache	22
Neck pain	33
Dizziness	21
Horner syndrome	3
Diplopia	7
Cerebellar signs	13
NIHSS score (mean, range)	1.1 ± 1.9 (0–9)
Imaging	
Stroke on DWI	14
Onset-to-HR-MR imaging delay (day, mean, range)	8.6 ± 6.0 (3–16)
Clinical follow-up (month, mean, range)	9.6 ± 3.6 (6–32)
Imaging follow-up (month, mean, range)	7.4 ± 6.3 (4–32)

Table 2: Comparison of neurologists' and HR-MR classifications

HR-MR imaging classification	Neurologists' Classifications		Total
	VAD	No VAD	
VAD	14	4	18
No VAD	4	13	17
Total	18	17	35

bral venous plexus (Fig 2). In these 4 patients, no supportive evidence of VAD was visible on imaging follow-up because the initial lumen patency (3 occlusions and 1 irregularity) and fat-suppressed T1WI sequences remained unchanged (follow-up range, 19–32 months).

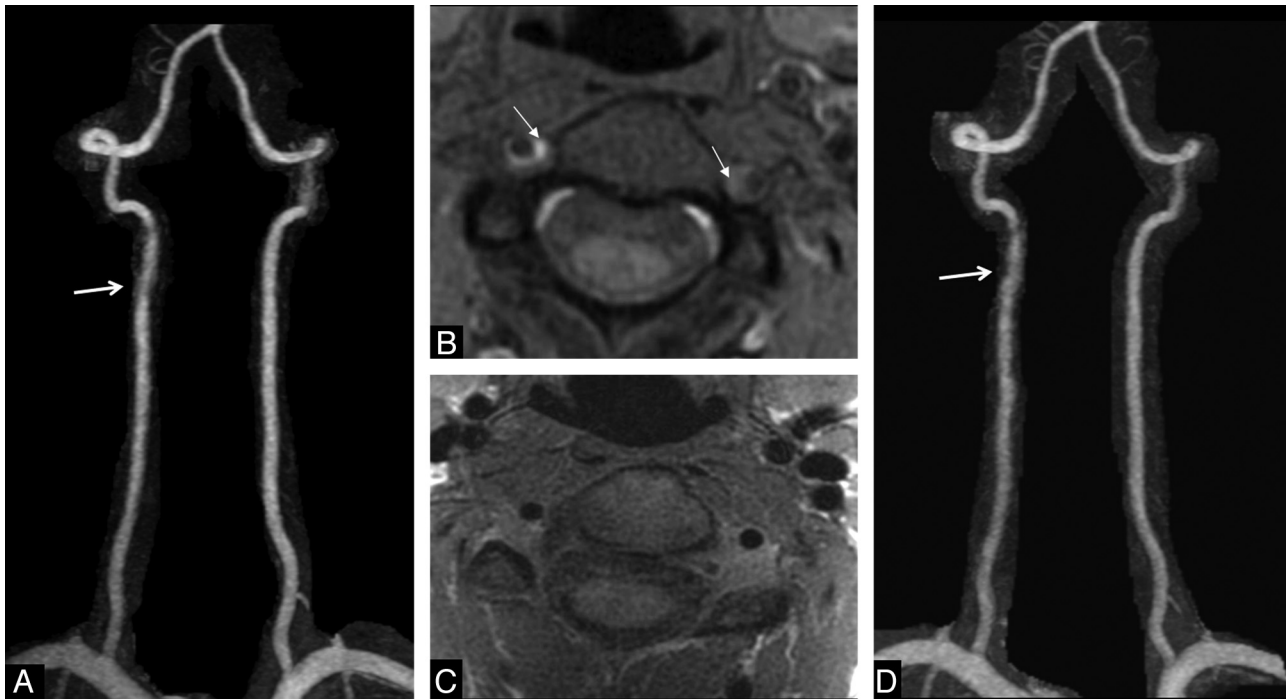


Fig 2. Example of discordance between the standard approach and HR-MR imaging. Suspicion of traumatic right acute VA dissection in a 25-year-old woman with sudden neck pain and dizziness, without stroke. DUS findings were consistent with a right vertebral mural hematoma (not shown). *A*, On CE-MRA, note irregularity of the right V2 segment (arrow). *B*, On axial fat-suppressed cervical T1WI, note hyperintense crescentic thickening of the right VA, associated with a slight crescentic hyperintensity of the left VA (arrows). *C*, On axial high-resolution T1WI, obtained 24 hours later, the crescentic hyperintense mural thickening is no longer present, leading to the diagnosis of inflow enhancement of the hypertrophic venous structure. *D*, On 6-month follow-up CE-MRA, the lumen of the right VA remains unchanged (arrow).

In 4 of the 17 patients in group B, HR-MR imaging findings were considered abnormal, showing a clear mural hematoma, which in 3 cases affected V3 segments and in 1 case, the V2 segment (Figs 3 and 4). In these 4 cases, follow-up imaging favored VAD because it showed a progressive normalization of the initial stenosis on CE-MRA.

Discussion

The main result of the present study is the added diagnostic value of HR-MR imaging in patients with suspected VAD and doubtful or discordant standard imaging. The addition of HR-MR imaging modified the diagnosis in 8 of 35 patients. For the diagnosis of VAD, noninvasive vascular imaging techniques are used though all have limitations. While DUS frequently demonstrates hemodynamic abnormalities in VAD, specific signs of dissection are lacking in >80% of cases⁶ due to shadowing from the adjacent transverse processes and limited visibility of the distal extradural segment of the VA. Thus, in patients with suspected VAD and negative findings on DUS, other diagnostic imaging tools are necessary. Multidetector CT angiography was shown to have high sensitivity and specificity for the diagnosis of VAD.⁷ However, the accuracy of CT in the evaluation of acute ischemic lesions in the posterior cranial fossa remains limited.¹⁵ Therefore, MR imaging is the preferred imaging technique to search, in the same examination, for stroke and for a specific aspect of cervical artery dissection (ie, the mural hematoma). Hypertrophy of the venous plexus that surrounds the VA is the main source of misdiagnosis on MR imaging. Venous blood in the transverse canal flows through a compartmentalized crescentic space formed by the periosteum and by fibrous leaflets around the artery.¹⁶

The resulting flow-related enhancement of the venous plexus gives a hyperintense signal intensity on standard fat-suppressed T1WI and can mimic the shape and the bright signal intensity of a mural hematoma, despite the use of a saturation pulse technique.^{17,18}

False-positive results on fat-suppressed T1WI, attributable to a misinterpretation of the high-signal intensity of veins, are frequent, especially in a small nondominant VA. In the current study, 4 patients were categorized as having a dissection, whereas this was unlikely given that HR-MR imaging failed to demonstrate a mural hematoma and lumen patency was unchanged on CE-MRA follow-up. All these presumed false-positive cases presented a crescentic hyperintense mural thickening on axial fat-suppressed T2WI and PDWI sequences, without low signal intensity of the intimal layer between the lumen and the crescentic hyperintense mural thickening on the TOF sequence; furthermore, the signal intensity was similar to that of the sternocleidomastoid muscle on T1WI, leading to the diagnosis of inflow enhancement of the hypertrophic venous structure.

The tortuosity and axial course of the V3 segment account for a large number of false-negative findings on standard axial fat-suppressed T1WI sequences. In the current study, a mural hematoma of the V3 segment was undiagnosed on both DUS and the fat-suppressed T1WI sequence in 3 patients but was clearly demonstrated on HR-MR imaging, by using coronal and sagittal section planes. In all cases, the crescentic hyperintense wall thickening was associated with a marked signal-intensity loss of the layer between the lumen and the crescentic hyperintense mural thickening on the TOF sequence. This pattern, also reported in carotid and aortic dissections, is sup-

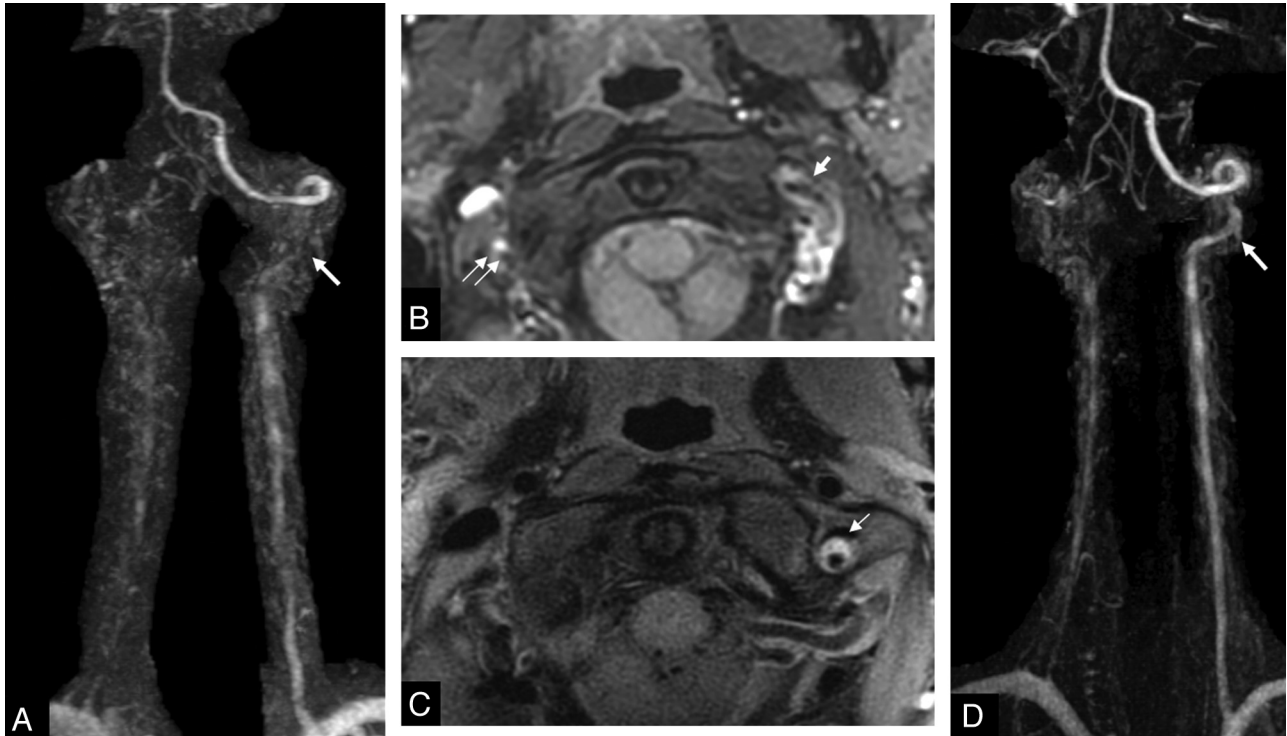


Fig 3. Example of discordance between the standard approach and HR-MR imaging. Suspicion of spontaneous acute dissection in a 40-year-old woman with left neck pain and laterobulbar acute stroke. *A*, On CE-MRA, note occlusion of the right VA and stenosis (arrow) of the left V3 segment. *B*, On axial fat-suppressed cervical T1WI, note inconclusive crescentic hyperintense mural thickening of the left VA (arrow) and a hyperintense occluded lumen of the right V3 segment (double arrow). DUS did not demonstrate any mural hematoma (not shown). *C*, On axial high-resolution fat-suppressed T2WI, obtained 24 hours later, note crescentic hyperintense mural thickening (arrow). *D*, On 5-month follow-up CE-MRA, note clear improvement of the left V3 stenosis. This favors the diagnosis of VAD.

posedly explained by magnetic susceptibility artifacts observed in cases of recent bleeding.^{14,19,20} On CE-MRA follow-up, the lumen became normal in all patients, in 1 case with an initial stenosis of the V2-V3 segment and in 3 cases with slight nonstenotic irregularities of the V3 segments.

Several limitations may have affected our results, in addition to the sources of potential bias inherent in retrospective reviews of cases. First, in this comparative accuracy study, the accuracy of the test under evaluation (HR-MR imaging) was not compared with the criterion standard (ie, conventional angiography). When a vertebral dissection is suspected, DSA rarely shows specific signs of VAD in cases of occlusion, stenosis, or normal lumen. For these reasons, DSA was not used in almost all cases, even in situations where the diagnosis was uncertain, and is progressively being replaced by noninvasive imaging modalities.⁴ Thus, the ability to assess noninvasive diagnostic-technique performance without the use of a criterion standard is of considerable interest. There is no universally accepted solution in diagnostic research when faced with the absence of a criterion standard. In such a case, an alternative approach involves plotting the results obtained with the new technique versus those obtained with a more established technique.

In accordance with a recent review of solutions for diagnostic accuracy studies with an imperfect or missing criterion standard,²¹ we constructed a reference standard (neurologic classification) based on multiple pieces of information (imaging and clinical tests). Thus, as suggested by Rutjes et al,²² not only discordant but also concordant results were retested with the new criterion standard (evolution on follow-up CE-MRA

and standard fat-suppressed T1WI), which is close to everyday practice. Second, CT angiography was not part of the standard etiologic work-up in our institution. However, it would be interesting to compare CE-MRA and CT angiography accuracy in discordant cases because the sensitivity of the latter for the diagnosis of VAD seems to be high, even in cases of normal lumen diameter.²³ Third, we deliberately excluded patients with normal lumen on CE-MRA because of the difficulty in choosing the position of the HR-MR imaging sections. This exclusion could be a source of bias and minimizes the generalizability of our results. Similarly, we arbitrarily chose to consider patients with unchanged VA occlusion as non-VAD patients. A longer monitoring period might have shown late recanalization, though Arauz et al²⁴ recently demonstrated that recanalization of VAD occurs mainly within the first 6 months after the onset of symptoms, even in the case of occlusion. Finally, in the case of multiple VADs (2 patients), we chose to consider only the symptomatic VAD, given that the treatment does not depend on the number of dissected vessels, and to avoid an artificial increase in the population. However, this choice may lead to a potential bias of selection in those patients.

Conclusions

VAD represents a diagnostic challenge. In patients referred with suspected dissection, it is not rare for the initial DUS and standard fat-suppressed T1WI to be inconclusive. VAD then remains presumptive, and treatment is initiated without a definite diagnosis. In patients with a high suspicion of VAD and discordant or doubtful baseline DUS and MR imaging find-

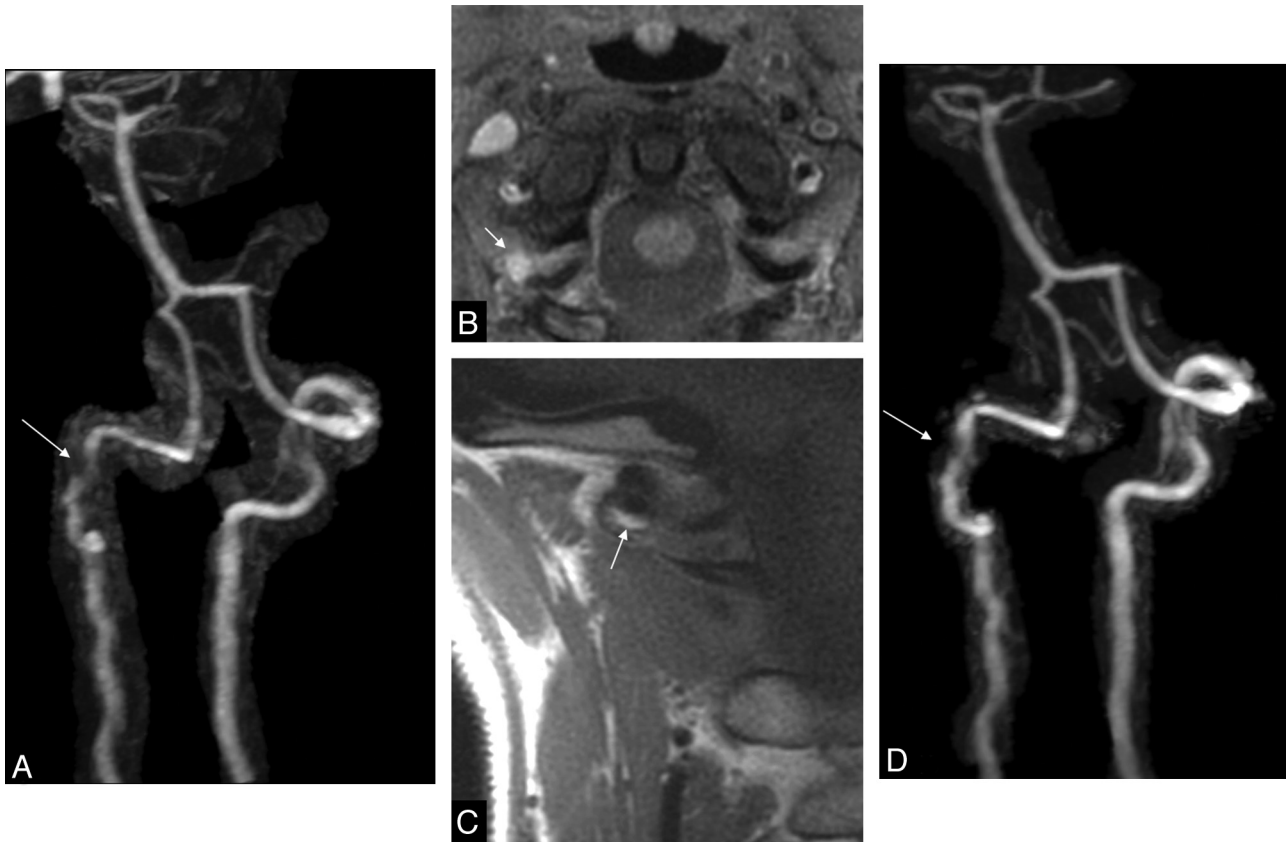


Fig 4. Example of discordance between the standard approach and HR-MR imaging. Suspicion of spontaneous acute dissection in a 47-year-old woman with postchiropractic right neck pain and transient dizziness, without stroke. Findings of DUS were inconclusive (not shown). *B*, On standard axial fat-suppressed cervical T1WI, note nonspecific hyperintense crescentic mural thickening of the right V3 segment (arrows). *A* and *D*, On CE-MRA, note stenosis (arrow, *A*) of the right V3 segment, which was partially resolved on 1-year follow-up CE-MRA (*D*, arrow). *C*, Coronal high-resolution T1WI, obtained 24 hours after CE-MRA, demonstrates a clear hyperintense crescentic mural thickening of the right V3 segment (arrow). This supports the diagnosis of VAD.

ings, our results encourage the use of HR-MR imaging as a second-line screening tool.

References

- Caplan LR. Dissections of brain-supplying arteries. *Nat Clin Pract Neurol* 2008;4:34–42
- Iwase H, Kobayashi M, Kurata A, et al. Clinically unidentified dissection of vertebral artery as a cause of cerebellar infarction. *Stroke* 2001;32:1422–24
- Schievink WI. Spontaneous dissection of the carotid and vertebral arteries. *N Engl J Med* 2001;344:898–906
- Debette S, Leys D. Cervical-artery dissections: predisposing factors, diagnosis, and outcome. *Lancet Neurol* 2009;8:668–78
- Engelter ST, Brandt T, Debette S, et al. Antiplatelets versus anticoagulation in cervical artery dissection. *Stroke* 2007;38:2605–11
- Dittrich R, Dziewas R, Ritter MA, et al. Negative ultrasound findings in patients with cervical artery dissection: negative ultrasound in CAD. *J Neurol* 2006;253:424–33
- Vertinsky AT, Schwartz NE, Fischbein NJ, et al. Comparison of multidetector CT angiography and MR imaging of cervical artery dissection. *AJNR Am J Neuroradiol* 2008;29:1753–60
- Leclerc X, Lucas C, Godefroy O, et al. Preliminary experience using contrast-enhanced MR angiography to assess vertebral artery structure for the follow-up of suspected dissection. *AJNR Am J Neuroradiol* 1999;20:1482–90
- Oppenheim C, Naggara O, Touze E, et al. High-resolution MR imaging of the cervical arterial wall: what the radiologist needs to know. *Radiographics* 2009;29:1413–31
- Naggara O, Touze E, Marsico R, et al. High-resolution MR imaging of periarterial edema associated with biological inflammation in spontaneous carotid dissection. *Eur Radiol* 2009;19:2255–60
- Bachmann R, Nassenstein I, Kooijman H, et al. Spontaneous acute dissection of the internal carotid artery: high-resolution magnetic resonance imaging at 3.0 Tesla with a dedicated surface coil. *Invest Radiol* 2006;41:105–11
- Bachmann R, Nassenstein I, Kooijman H, et al. High-resolution magnetic resonance imaging (MRI) at 3.0 Tesla in the short-term follow-up of patients with proven cervical artery dissection. *Invest Radiol* 2007;42:460–66
- Naggara O, Oppenheim C, Toussaint JF, et al. Asymptomatic spontaneous acute vertebral artery dissection: diagnosis by high-resolution magnetic resonance images with a dedicated surface coil. *Eur Radiol* 2007;17:2434–35
- Flis CM, Jager HR, Sidhu PS. Carotid and vertebral artery dissections: clinical aspects, imaging features and endovascular treatment. *Eur Radiol* 2007;17:820–34
- Chen CJ, Tseng YC, Lee TH, et al. Multisection CT angiography compared with catheter angiography in diagnosing vertebral artery dissection. *AJNR Am J Neuroradiol* 2004;25:769–74
- Palombi O, Fuentes S, Chaffanjon P, et al. Cervical venous organization in the transverse foramen. *Surg Radiol Anat* 2006;28:66–70
- Miaux Y, Cognard C, Martin-Duverneuil N, et al. Flow-related enhancement in the vertebral plexus mimicking an intramural hematoma. *AJNR Am J Neuroradiol* 1996;17:191–92
- Dumas JL, Stanescu R, Goldlust D, et al. Vertebral vein imaging with MR angiography. *AJNR Am J Neuroradiol* 1997;18:1190–92
- Litmanovich D, Bankier AA, Cantin L, et al. CT and MRI in diseases of the aorta. *AJR Am J Roentgenol* 2009;193:928–40
- Buckley O, Rybicki FJ, Gerson DS, et al. Imaging features of intramural hematoma of the aorta. *Int J Cardiovasc Imaging* 2010;26:65–76
- Reitsma JB, Rutjes AW, Khan KS, et al. A review of solutions for diagnostic accuracy studies with an imperfect or missing reference standard. *J Clin Epidemiol* 2009;62:797–806
- Rutjes AW, Reitsma JB, Coomarasamy A, et al. Evaluation of diagnostic tests when there is no gold standard: a review of methods. *Health Technol Assess* 2007;11:iii, ix–51
- Lum C, Chakraborty S, Schlossmacher M, et al. Vertebral artery dissection with a normal-appearing lumen at multisection CT angiography: the importance of identifying wall hematoma. *AJNR Am J Neuroradiol* 2009;30:787–92
- Arauz A, Marquez JM, Artigas C, et al. Recanalization of vertebral artery dissection. *Stroke* 2010;41:717–21. Epub 2010 Feb 11